JOURNAL OF SOLID STATE CHEMISTRY 99, 63–71 (1992)

Crystallographic Data, Vibrational Spectra, and Magnetic Properties of the Two Polymorphic Forms of Tm_2BaNiO_5

A. SALINAS-SÁNCHEZ, R. SÁEZ-PUCHE,* AND F. FERNÁNDEZ

Departamento Química Inorgánica, Facultad de Químicas, UCM, 28040-Madrid, Spain

A. DE ANDRÉS

Instituto de Ciencia de Materiales de Madrid, C.S.I.C., Universidad Autónoma, Departamento de Física Aplicada C-IV, 28049-Madrid, Spain

A. E. LAVAT

Area de Química, Facultad de Ingeniería, Universidad Nacional del Centro de la Provincia de Buenos Aires,7400 Olavarría, Argentina

AND E. J. BARAN

Departamento de Química, Universidad Nacional de La Plata, 1900-La Plata, Argentina

Received September 24, 1991; in revised form December 2, 1991; accepted December 23, 1991

The new brown-tobacco-colored Tm_2BaNiO_5 oxide has been prepared and the X-ray diffraction study reveals that it crystallizes with the Sm_2BaCuO_5 structural type, space group *Pnma* and lattice parameters of $a = 12.1939(2)$ Å, $b = 5.6555(1)$ Å, and $c = 6.9745(1)$ Å. When this oxide is heated in air at 1600 K for 12 hr it changes to give the known dark-green-colored oxide, which belongs to the Nd_2BaNiO_5 structure type, space group *Immm*. We have also characterized the new low-temperature phase, LT-*Pnma*, and the high-temperature phase, HT-*Immm*, using both Raman and infrared spectroscopy techniques. Magnetic susceptibility data reveal the existence of 1D-antiferromagnetic order above room temperature for the HT-Tm_2BaNiO_5. The maximum observed in the magnetic susceptibility at 8.3 K has been attributed to the existence of 3D-antiferromagnetic ordering in both nickel and thulium sublattices. However, we have not found any magnetic ordering down to 4.2 K for the LT-Tm_2BaNiO_5 oxide.

Introduction

The first member, Nd_2BaNiO_5, of the new family of R_2BaNiO_5 oxides (R = Nd–Tm and Y) was synthesized and characterized by Schiffler and Müller-Buschbaum (*1*, *2*). These oxides crystallize with orthorhombic symmetry, space group *Immm*, showing as main structural feature the existence of isolated chains of NiO_6 corner-sharing flattened octahedra along the *a*-axis, Fig. 1a, giving rise to very short Ni–O(axial)–Ni distances

* To whom correspondence should be addressed.

0022-4596/92 $5.00

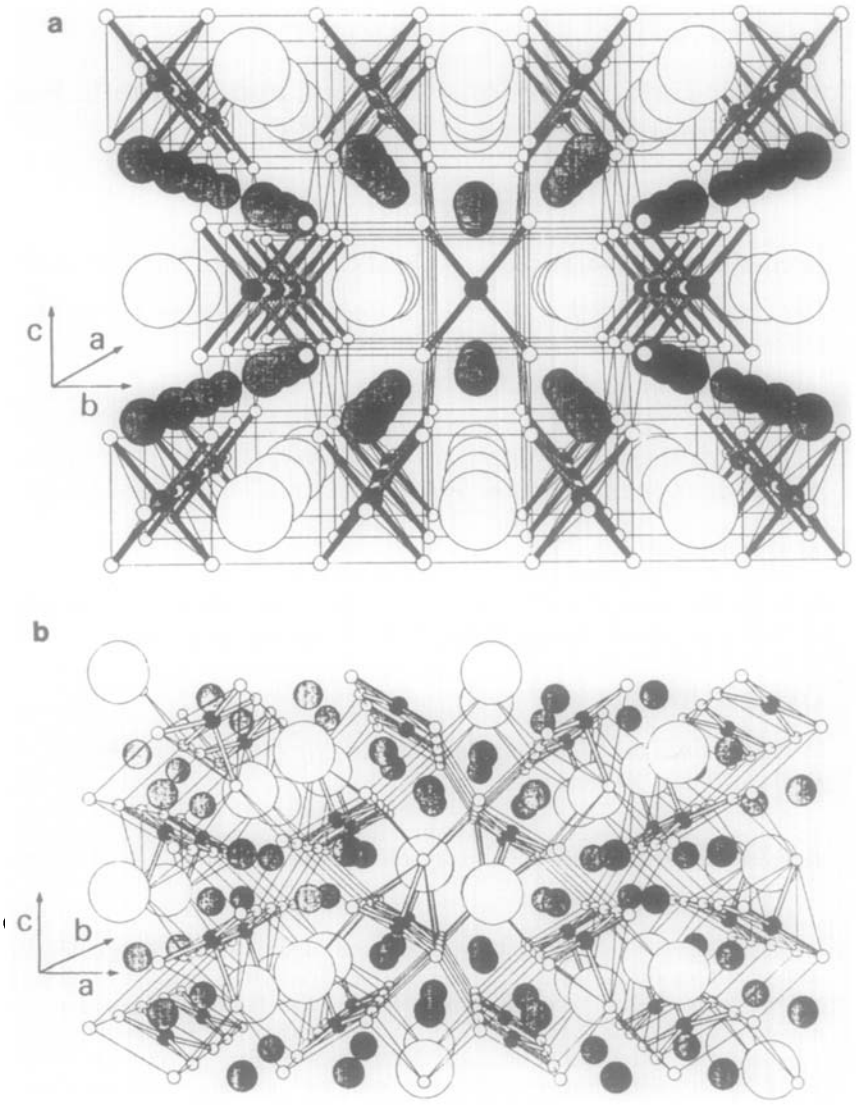

FIG. 1. (a) Perspective view, along the *a* axis, of HT-Tm_2BaNiO_5 showing the vertex-sharing chains of flattened NiO_6 octahedra. (b) Crystal structure of LT-Tm_2BaNiO_5 showing the isolated square pyramids of NiO_5. The larger circles represent the barium atoms, the medium dotted are the thulium atoms, and the black circles are the nickel atoms.

(3.765 Å for Tm_2BaNiO_5 (*3*)). This justifies the 1D-antiferromagnetic behavior above room temperature that we have reported earlier for Y_2BaNiO_5 (*4*). Although this one-dimensional order has been detected for the different R_2BaNiO_5 oxides, it is strongly masked by the paramagnetism of the R^{+3} ions (*5*). Moreover, magnetic susceptibility measurements and neutron diffraction studies have revealed the existence of 3D-antiferromagnetic order in both R^{+3} and Ni^{+2} sublattices at low temperatures (*5*, *6*).

Very recently, using neutron diffraction, we have reported the existence of a new low-temperature phase (LT) for Tm_2BaNiO_5 which shows the Sm_2BaCuO_5 structural type with orthorhombic symmetry, space group *Pnma* (*3*).

In this paper, the known high-temperature (HT) and the low-temperature (LT) forms have been extensively characterized using X-ray diffraction, IR, and Raman techniques. The study of the magnetic properties of both phases has been also considered.

Experimental

The low-temperature form, LT-Tm_2BaNiO_5, was obtained by heating in air the stoichiometric amounts of high purity oxides Tm_2O_3 (99.999%), NiO (99.99%), and $BaCO_3$ (R.A.), for 24 hr at 1273 K. Subsequent thermal treatments at 1473 K, with some interruptions for grinding to improve the homogeneity of the sample, yield a brown-tobacco-colored powder, and the X-ray diffraction data reveal that it shows the Sm_2BaCuO_5 structural type (*3*) (Fig. 1b). Further thermal treatment in air at 1600 K for 12 hr yields a green-colored powder with the structure previously reported for Tm_2BaNiO_5 oxide (*2*). Annealing of this HT-Tm_2BaNiO_5 form at 1473 K does not yield the LT-Tm_2BaNiO_5 form, and the HT-*Immm* phase remains stable.

X-ray powder diffraction patterns were recorded using a Siemens Kristalloflex 810 diffratometer and a D-500 goniometer provided with a graphite monochromator and Cu$K\alpha$ radiation. Diffraction data were collected by step scanning over an angular range of $10° < 2\theta < 120°$ in increments of 0.04° and a counting time of 15 sec for step. The data were analyzed with the Rietveld method using the FULLPROF program (*7*). A pseudo-Voight profile-function without cristallites preferred orientation was used.

The IR spectra were recorded with a Perkin–Elmer 580 B Spectrophotometer using the KBr-pellet technique. Raman spectra were obtained with an X–Y Dilor multichannel spectrometer using the 488-nm line of an Ar-ion laser for excitation.

Magnetic susceptibility measurements were made using a fully automatic DSM8 magneto-susceptometer based on the Faraday method in the temperature range 300–4.2 K. The magnetic field used was 6.5 kG with $H\ dH/dz = 14.2\ kG^2\ cm^{-1}$. The setup was calibrated with $Hg[Co(SCN)_4]$ and $Gd_2(SO_4)_3 \cdot 8H_2O$ as standards, and no corrections were made for the ionic diamagnetism.

Results and Discussion

Crystallographic Data

Figures 2a and 2b show the observed and calculated X-ray diffraction patterns for the new LT-Tm_2BaNiO_5 (*Pnma*) oxide and the HT-Tm_2BaNiO_5 (*Immm*) described earlier (*2*). From the multiphase Rietveld refinement of both structures, an increase can be observed in the amount of unreacted Tm_2O_3 for the HT form, probably due to a small loss of NiO at the high temperature that is necessary to prepare this HT-Tm_2BaNiO_5 oxide. The refined atomic coordinates, bond length, and lattice parameters, which are $a = 12.1939(2)$ Å, $b = 5.6555(1)$ Å, and $c = 6.9745(1)$ Å for the HT-Tm_2BaNiO_5, fully agree with those reported earlier for this phase (*2, 3*).

Table I shows the structural parameters refined from the X-ray powder diffraction patterns for the new LT-Tm_2BaNiO_5 oxide. As was expected in the structure of the LT-Tm_2BaNiO_5 oxide, Fig. 1b and Table I, there are two thulium atoms in the unit cell, namely Tm(1) and Tm(2), situated in two different slightly distorted monocapped trigonal prisms sharing a triangular face formed by one O(3) and two O(2). These Tm_2O_{11} units are connected through edge-sharing giving rise to the three-dimensional network

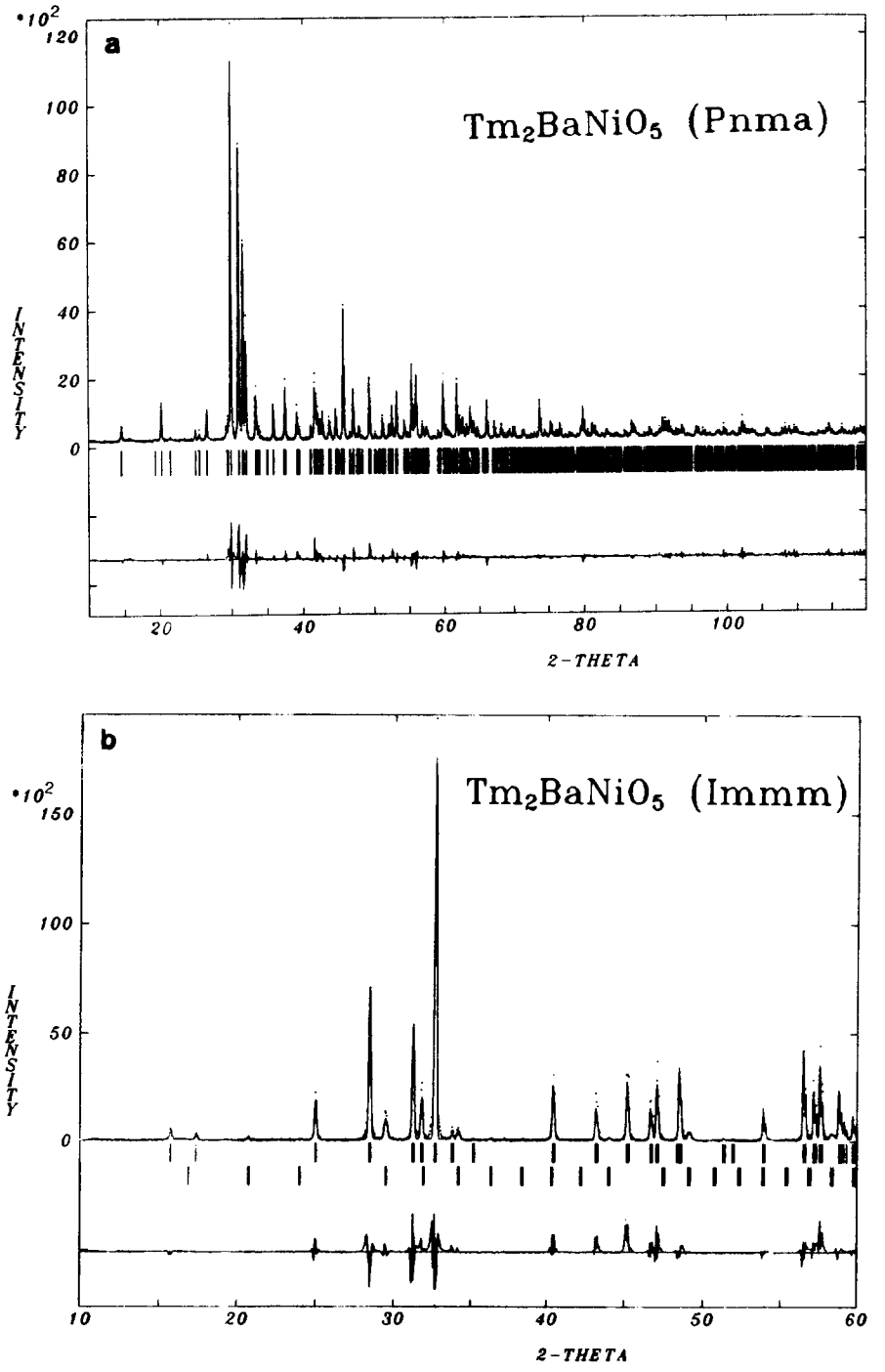

FIG. 2. Obtained and calculated X-ray diffraction patterns of both LT-Tm_2BaNiO_5 (a) and HT-Tm_2BaNiO_5 (b) forms at room temperature. Vertical marks show the position of allowed reflections. The difference curve is also plotted at the bottom of the figures. In (b) the allowed reflections of Tm_2O_3 are included in the refinement as the second row of vertical marks.

TABLE I

STRUCTURAL PARAMETERS FOR LT-Tm_2BaNiO_5, S. G. *Pnma*, $Z = 4$, $a = 12.1939(2)$ Å, $b = 5.6555(1)$ Å, $c = 6.9704(1)$ Å

Atom	Site	x/a	y/b	z/c
Ba	4*c*	0.9038(3)	¼	0.9227(5)
Tm(1)	4*c*	0.2930(2)	¼	0.1244(5)
Tm(2)	4*c*	0.0735(3)	¼	0.4005(4)
Ni	4*c*	0.6553(7)	¼	0.699(1)
O(1)	8*d*	0.423(2)	−0.013(4)	0.180(3)
O(2)	8*d*	0.234(2)	0.507(4)	0.355(3)
O(3)	4*c*	0.094(3)	¼	0.064(4)

Note. Overall temperature factor = 0.26(4) Å^2; R_P = 19.7, R_{WP} = 20.2, R_{EXP} = 9.61, χ^2 = 4.40, R_B = 8.23; No. of reflections = 791.

shown in Fig. 1b. The nickel is situated in a distorted square pyramidal environment, since the O(3) is the apex of the pyramid yielding the shortest Ni–O(3) distance about 2% smaller than the two other Ni–O(1) and Ni–O(2) basal distances, while in the case of the isostructural Ln_2BaCuO_5 oxides this Cu–O(3) distance is about 10% larger than the other four (*8*, *9*). In a previous work we attempted to look for the structural relationship between the LT → HT forms of Tm_2BaNiO_5 (*3*). However, we have not yet found a simple way to describe this low- to high-temperature complex phase transition, for which even strong displacements of the heavy atoms have been observed.

Vibrational Spectra

The vibrational spectroscopic behavior also allows one to differentiate unambiguously the two polymorphic forms of Tm_2BaNiO_5. The spectra can be discussed briefly, as follows:

LT form. The IR spectrum of this form is shown in Fig. 3. It presents the same characteristic as the well known Ln_2BaCuO_5 "green phases," for which vibrational behavior has been discussed recently (*10*).

Despite the fact that in the present case the Ni–O apical distance is slightly shorter than the four equatorial ones, whereas in the copper containing phases the inverse situation holds, as we stated earlier, the spectra are practically identical with the exception of an intensity inversion between the two components of the first two strong and broad doublets, located at ca. 500 and 400 cm^{-1}, respectively, in Tm_2BaNiO_5.

An approximate assignment of this spectrum, based in the arguments previously advanced (*10*), can be proposed as follows:

—The weak IR shoulder at 595 cm^{-1} can be assigned to the Ni–O apical stretching, because this is the shortest and, consequently, strongest bond.

—The first broad doublet, with components at 501 and 451 cm^{-1}, may represent the symmetric and antisymmetric stretching modes of the basal NiO_4 units.

—The remaining bands are more difficult assign; they are surely strongly mixed modes, and include bending of the NiO_5 moieties, coupled with the vibrational

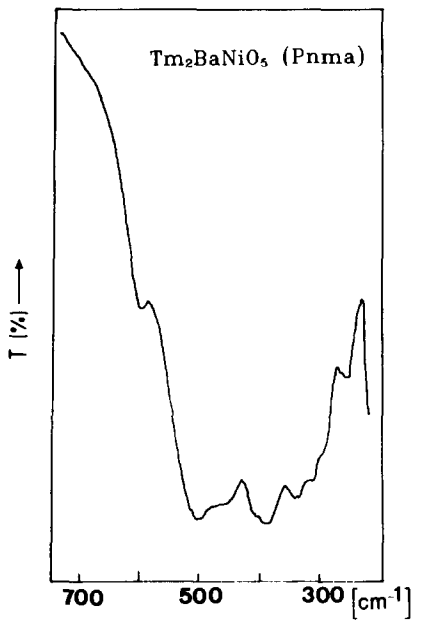

FIG. 3. Infrared spectrum of LT-Tm_2BaNiO_5.

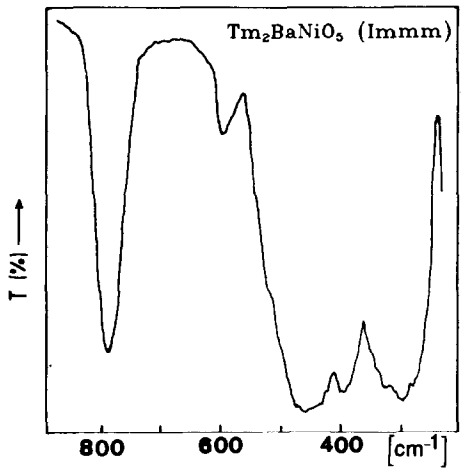

FIG. 4. Infrared spectrum of HT-Tm_2BaNiO_5.

modes of the other metal–oxygen polyhedra present in the lattice. These bands are located at 400, 389, 332, 311, 291 (sh), 251, and 210 cm^{-1}.

The Raman spectrum of this modification, although not so well defined as in the case of the copper compounds (*10*), shows also striking similarities to the spectra of these materials.

HT form. As in the case of all other materials possessing this structural type, the IR spectrum is dominated by a very strong and unusually high-frequency band, lying above 700 cm^{-1} (*11*), as can be seen in Fig. 4.

Raman spectra of phases of this type have not been so far reported but, as our study has shown, they are also very characteristic. In Fig. 5, we present this spectrum for the HT form of Tm_2BaNiO_5. The measured frequencies in both the IR and Raman spectra are compared in Table II. The Raman modes involve only two kind of ions (the Tm and the oxygen of the NiO_4 planes), the other ions (apical oxygens, Ba, and Ni) being at inversion centers.

The Tm atomic mass is 10 times that of oxygen, so one expects that the Tm motions have frequencies quite lower than those of the oxygen modes. We can assign the two sharp peaks at low frequency to the Tm modes, while the other three, at higher frequencies, are related to oxygen motions.

The first strong IR band (786 cm^{-1}) can be related to the short and strong apical Ni–O bonds, but this mode is surely reinforced by coupling effects along the —Ni–O–Ni–O– chains, and the highest frequency Raman mode is probably due to the symmetric stretching of the equatorial NiO_4 bonds.

The IR and Raman peaks in the 600 to 300 cm^{-1} region can probably be, all of them, oxygen motions.

Magnetic Behavior of the LT and HT Forms of Tm_2BaNiO_5

Figures 6 and 7 show the temperature variation of the magnetic susceptibility for both HT- and LT-Tm_2BaNiO_5 oxides, respectively. It can be observed that the susceptibility of LT-Tm_2BaNiO_5 follows a Curie–Weiss behavior in the 300–8 K temperature range, and the experimental magnetic moment obtained for Tm^{+3} taking into account the nickel contribution with $S = 1$ is 7.53 BM, which fairly agrees with that expected for isolated ground term $^3H_6$ of Tm^{+3} (*12*). Both the slight deviation downward from linearity observed in the χ^{-1} vs T plot and the negative value of the Weiss constant, -12.5 K, can be attributed to the crystal field effect, and it is not necessary claim the existence of antiferromagnetism to explain this behavior (*13*).

Neutron diffraction studies confirm the absence of antiferromagnetic interactions down to 1.5 K for this LT form (*14*). It is worth noting that the absence of antiferromagnetism for both this LT form and for the isostructural "green phase" Tm_2BaCuO_5 (*15*) appear to be a characteristic behavior due to the ground crystal field term of Tm^{+3}.

Figure 7 shows the variation of the molar magnetic susceptibility with the temperature for LT-Tm_2BaNiO_5 oxide. It can be observed that the susceptibility obeys a

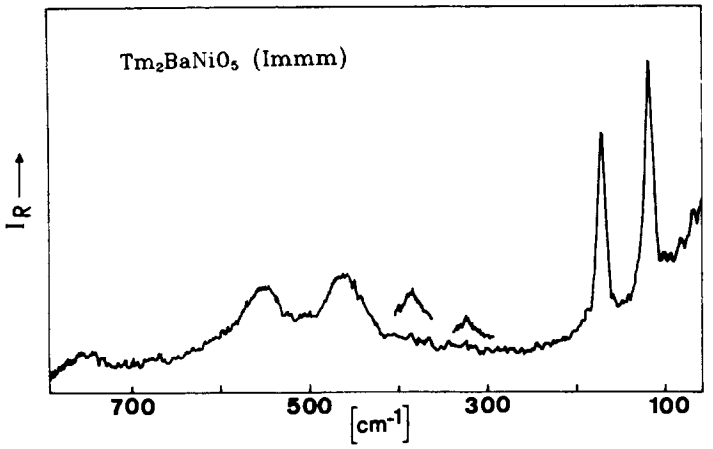

FIG. 5. Raman spectrum of HT-Tm_2BaNiO_5.

Curie–Weiss law between 300 and 60 K, and the obtained magnetic moment of 7.70 BM agrees with that expected for Tm^{+3}. This behavior can be explained considering the structure of this HT form, Fig. 1a; as we stated earlier, the existence of a one-dimensional arrangement of vertex-sharing NiO_6 flattened octahedra, giving rise to a very short Ni–O–Ni distance at 180°, will enhance the 1D-superexchange interactions in the nickel sublattice. Recently it has been reported that these interactions are operative above room temperature in the case of the isostructural Y_2BaNiO_5 (*4*). Since the Ni–O–Ni distance and angle remain almost constant for all the members of the family of R_2BaNiO_5 oxides, it is expected that these 1D-antiferromagnetic interactions will be also operative for this HT-Tm_2BaNiO_5 at about the same temperature, although they are masked by the strong paramagnetic signal due to the Tm^{+3} contribution. This explains the lack of a Ni^{+2} contribution to the susceptibility below 300K as we have discussed above. At 8.3 K a net maximum is observed in the χ vs T plot, Fig. 7, which can be attributed to a 3D-antiferromagnetic ordering in both the Ni and Tm sublattices. This behavior has been confirmed in a previous work from neutron diffraction scattering (*14*).

In summary, the different magnetic behavior found for these LT and HT forms of Tm_2BaNiO_5 is a consequence of the very different structural features that these oxides show. In the case of HT-Tm_2BaNiO_5 the superexchange interactions are greatly favorable due to the very short Ni–O–Ni distances at 180°. For the LT form the pathways for these interactions in the nickel sub-

TABLE II

COMPARISON OF THE INFRARED AND RAMAN SPECTRA OF THE HT FORM OF Tm_2BaNiO_5 (VALUES IN cm^{-1})

IR	Raman
786 vs	760 w, br
592 w	550 s
455 vs, br	460 s
388 s	~ 390 vw, br
292 vs, br	~ 310 vs, br
—	170 vs
—	120 vs

Note. vs, very strong; s, strong; w, weak; vw, very weak; br, broad.

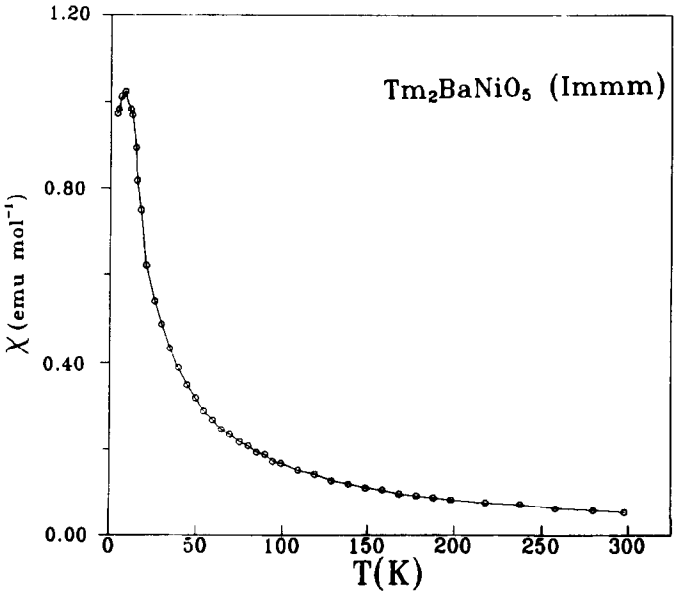

FIG. 6. Temperature dependence of the molar magnetic susceptibility for HT-Tm_2BaNiO_5.

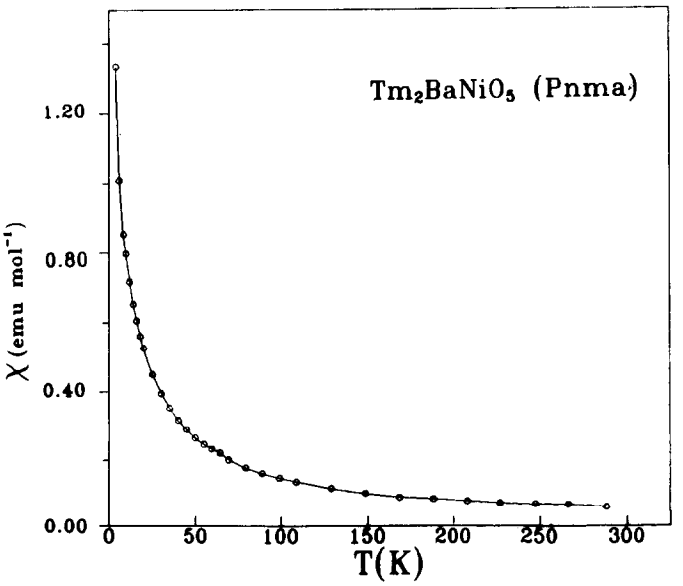

FIG. 7. Temperature dependence of the molar magnetic susceptibility for LT-Tm_2BaNiO_5.

lattice are more complex, and at least two oxygen atoms are involved in the superexchange (Ni–O–Tm–O–Ni); also, the angle is very different away from 180°, as can be observed in Fig. 1b. These facts justify that the antiferromagnetic interactions are not operative down to 1.5 K.

Acknowledgments

The authors thank CICYT, Mat89-0768, and the Spanish MEC for financial support of the Spanish–Argentinan research project.

References

1. S. SCHIFFLER AND H. K. MÜLLER-BUSCHBAUM, *Z. Anorg. Allg. Chem.* **532,** 10 (1986).
2. S. SCHIFFLER AND H. K. MÜLLER-BUSCHBAUM, *Monast. Chem.* **118,** 741 (1987).
3. A. SALINAS-SÁNCHEZ, R. SÁEZ-PUCHE, J. RODRIGUEZ-CARVAJAL, AND J. L. MARTINEZ, *Solid State Commun.* **78(6),** 481 (1991).
4. R. SÁEZ-PUCHE, J. M. CORONADO, C. L. OTERO-DIAZ, AND J. M. MARTIN-LLORENTE, *J. Solid State Chem.* **93,** 461 (1991).
5. J. AMADOR, E. GUTIERREZ-PUEBLA, M. A. MONGE, I. RASINES, F. FERNANDEZ, C. RUIZ-VALERO, R. SÁEZ-PUCHE, AND J. A. CAMPA, *Phys. Rev. B* **42,** 7918, (1990).
6. J. A. ALONSO, J. AMADOR, J. L. MARTINEZ, I. RASINES, J. RODRIGUEZ-CARVAJAL, AND R. SÁEZ-PUCHE, *Solid State Commun.* **76,** 467 (1990).
7. J. RODRIGUEZ-CARVAJAL, *in* "Abstracts of the Satellite Meeting on Powder Diffraction on the XVth Congress of the International Union of Crystallography, Toulouse, 1990," p 127.
8. A. SÁLINAS-SANCHEZ *et al.*, in preparation.
9. R. NORRESTAM, M. HJORTH, AND J. O. BOVIN, *Z. Kristallogr.* **183,** 245 (1988).
10. E. J. BARAN, G. P. CICILEO, G. PUNTE, A. E. LAVAT, AND M. TREZZA, *J. Mater. Sci. Lett.* **7,** 1010 (1988).
11. A. E. LAVAT *et al.*, in preparation.
12. J. H. VAN VLECK, "The Theory of Electric and Magnetic Susceptibilities," Oxford Univ. Press, Oxford (1965).
13. P. CARO, J. DEROUET, L. BEAURY, AND E. SOULIE, *J. Chem. Phys.* **70(15),** 2542 (1979).
14. A. SÁLINAS-SANCHEZ, R. SÁEZ-PUCHE, J. RODRIGUEZ-CARVAJAL, AND J. L. MARTINEZ, submitted for publication.
15. J. L. GARCIA, private communication.